3432 J. Phys. Chem. A **2006,** *110,* 3432−3446

Twisting Dynamics in the Excited Singlet State of Michler's Ketone

Jahur A. Mondal, Hirendra N. Ghosh, Tapan K. Ghanty, T. Mukherjee, and Dipak K. Palit*

Radiation & Photochemistry Division, Bhabha Atomic Research Centre, Trombay, Mumbai 400085, India

Received: September 29, 2005; In Final Form: December 17, 2005

Ultrafast relaxation dynamics of the excited singlet (S_1) state of Michler's ketone (MK) has been investigated in different kinds of solvents using a time-resolved absorption spectroscopic technique with 120 fs time resolution. This technique reveals that conversion of the locally excited (LE) state to the twisted intramolecular charge transfer (TICT) state because of twisting of the *N*,*N*-dimethylanilino groups with respect to the central carbonyl group is the major relaxation process responsible for the multi-exponential and probe-wavelength-dependent transient absorption dynamics of the S_1 state of MK, but solvation dynamics does not have a significant role in this process. Theoretical optimization of the ground-state geometry of MK shows that the dimethylanilino groups attached to the central carbonyl group are at a dihedral angle of about 51° with respect to each other because of steric interaction between the phenyl rings. Following photoexcitation of MK to its S_1 state, two kinds of twisting motions have been resolved. Immediately after photoexcitation, an ultrafast "anti-twisting" motion of the dimethylanilino groups brings back the pretwisted molecule to a near-planar geometry with high mesomeric interaction and intramolecular charge transfer (ICT) character. This motion is observed in all kinds of solvents. Additionally, in solvents of large polarity, the dimethylamino groups undergo further twisting to about 90° with respect to the phenyl ring, to which it is attached, leading to the conversion of the ICT state to the TICT state. Similar characteristics of the absorption spectra of the TICT state and the anion radical of MK establish the nearly pure electron transfer (ET) character of the TICT state. In aprotic solvents, because of the steep slope of the potential energy surface near the Franck−Condon (FC) or LE state region, the LE state is nearly nonemissive at room temperature and fluorescence emission is observed from only the ICT and TICT states. Alternatively, in protic solvents, because of an intermolecular hydrogen-bonding interaction between MK and the solvent, the LE region is more flat and stimulated emission from this state is also observed. However, a stronger hydrogen-bonding interaction between the TICT state and the solvent as well as the closeness between the two potential energy surfaces due to the TICT and the ground states cause the nonradiative coupling between these states to be very effective and, hence, cause the TICT state to be weakly emissive. The multi-exponentiality and strong wavelength-dependence of the kinetics of the relaxation process taking place in the S_1 state of MK have arisen for several reasons, such as strong overlapping of transient absorption and stimulated emission spectra of the LE, ICT, and TICT states, which are formed consecutively following photoexcitation of the molecule, as well as the fact that different probe wavelengths monitor different regions of the potential energy surface representing the twisting motion of the excited molecule.

1. Introduction

Photophysical and photochemical properties of the excited singlet (S_1) and triplet (T_1) states of 4,4′-bis-(*N*,*N*-dimethylamino)-benzophenone, which is popularly known as Michler's ketone (MK), have been the subject of extensive investigations during the last few decades.[1−10] Spectroscopic and photochemical properties of MK have been observed to be extremely sensitive to solvent characteristics. This has been attributed to the close proximity and solvent sensitivity of the relative positions of the energy levels of the lowest excited $n\pi^*$ and $\pi\pi^*$ states, both in the singlet and triplet manifold, as well as to the hydrogen-bonding ability of MK with the hydrogen-bond-donating solvents.[2,3] Different parameters, namely, polarity, hydrogen-bonding ability, and viscosity, which control the photophysical properties of MK, have been well characterized by different groups.[4−9]

Glasbeek and co-workers reported their results of femtosecond fluorescence up-conversion experiments on MK recently.[1,11] They showed that the fluorescence decay of MK is multiexponential and the lifetimes of the components are also dependent on the monitoring wavelength. The stokes shift of the maximum of the time-resolved fluorescence spectrum is anomalously fast and is accompanied by the concomitant decay of the intensity integrated over the time-resolved fluorescence band. The dynamic Stokes shift of the fluorescence maximum is normally interpreted as a result of solvation of the polar excited state.[12] If solvation is the only process responsible for the dynamic Stokes shift, then a concomitant decay of the integrated fluorescence intensity is not expected because the nature of the emissive state is not affected by the reorientation of the solvent molecules.[12] Hence, the authors explain that the anomalously fast dynamic Stokes shift is the result of two processes, namely, phenyl twisting and solvation, happening simultaneously. These are the two major processes that determine the relaxation dynamics of the S_1 state of MK.[1,11] However, the ultrafast

---

* To whom correspondence should be addressed. E-mail: dkpalit@apsara.barc.ernet.in.

10.1021/jp0555450 CCC: $33.50

fluorescence measurements could not provide any direct evidence in favor of the twisting dynamics and the time constants associated with the twisting process. Additionally, the dynamic Stokes shift, which was much faster than the average solvation time of the solvent, could also not be assigned to solvation dynamics in certainty. Moreover, the different lifetime components, which were recovered by analyzing the wavelength-dependent multiexponential fluorescence decay curves, were not assigned to specific processes or the transient species. Hence, although investigation using the ultrafast fluorescence spectroscopic technique has revealed some of the important features of the excited-state relaxation dynamics of MK, further studies are warranted to distinguish between the twisting motion and solvation dynamics as well as to assign the individual time constants to specific processes.

The time-resolved fluorescence and transient absorption spectroscopic techniques may be considered as two spectroscopic techniques that are complementary to each other. Each of them is capable of revealing some aspects of the dynamics but not all. Because the fluorescence spectroscopic technique applied by Glasbeek and co-workers could not reveal the complete microscopic dynamics of the S_1 state of MK, we got motivated to reinvestigate the excited-state dynamics of MK using femtosecond transient absorption spectroscopic technique. Amino-substituted benzophenones, including MK, are weakly fluorescent or nonfluorescent, and they have very short singlet state lifeteimes.[6,7,14,15] Hence, the ultrafast transient absorption spectroscopic technique may have a better edge over the fluorescence spectroscopic technique in investigation of the microscopic details of the relaxation dynamics of this class of molecules. The ultrafast absorption technique has been applied very successfully in the investigation of the dynamics of TICT processes in a few molecules[11,21−25] However, it is important to concede that for many large molecules the distinct treatment of ultrafast solvation and conformational relaxation dynamics is very complex. Because of the immense number of motional degrees of freedom, the characteristics of the total system of the solute and solvent molecules, solvation, and conformational relaxation often become highly competitive and a separate treatment of their dynamics is not meaningful.[11,18−25] In the present investigation, although the time-resolved absorption technique could resolve two kinds of twisting motions in the S_1 state of MK, no information regarding solvation of the state, despite its large polarity, could be obtained.

2. Experimental Section

MK from the Thomas-Becker triplet sensitizer kit was used after repeated recrystallization from methanol. All of the solvents used were of spectroscopic grade (Spectrochem, India) and used as received without further purification. Steady-state absorption spectra were recorded using a Shimadzu model UV-160A spectrophotometer. Fluorescence spectra were recorded using a Hitachi model 4010 spectrofluorimeter. Fluorescence spectra were corrected for the wavelength-dependence of the instrument response but not due to variation of refractive indices of the solvents. Fluorescence lifetimes were measured with 20-ps time resolution using a time-correlated single photon counting (TCSPC) spectrometer, the details of which are available in ref 26. For the present measurements, the third harmonic of a femtosecond Ti:Sapphire laser (i.e., 305 nm) has been used for excitation. High-purity-grade nitrogen gas (Indian Oxygen, purity >99.9%) was used to deaerate the samples whenever it was required.

Relaxation processes in the sub-500 ps time-domain were measured using a femtosecond pump−probe transient absorption spectrometer, which used a femtosecond Ti:Sapphire laser system supplied by CDP-Avesta, Russia. The laser system consisted of a Ti:Sapphire laser oscillator (model TISSA-50), which produced laser pulses of 6 nJ energy at 800 nm. These pulses were amplified in an optical amplifier (model MPA-50) to generate 50 fs laser pulses of about 300 μJ energy at a repetition rate of 1 kHz using the chirped pulse amplification (CPA) technique. The optical amplifier consists of a pulse stretcher, a multipass amplifier pumped by an intracavity frequency doubled Nd:YAG laser (6 W, 1 kHz) and a pulse compressor. Pump pulses at 400 nm were generated for excitation of the samples by frequency-doubling of one part of the 800 nm output of the amplifier in a 0.5 mm thick BBO crystal, and the other part of the amplifier output was used to generate the white light continuum (470−1000 nm) probe in a 2 mm thick sapphire plate. The direction of polarization of the pump beam was fixed at the magic angle. The sample solutions were kept flowing through a quartz cell of 1 mm path length. The probe beam was split into two equal parts, one of which passed through the excited zone of the sample to fall onto an integrating photodiode and the other part reached directly to another photodiode. For monitoring decay dynamics, a particular wavelength region with 10 nm bandwidth was selected using a pair of interference filters placed in front of the photodiodes. The variation of the relative intensities of the probe beams at different delay times with respect to the pump beam were monitored using the photodiodes coupled with the boxcar integrators. The overall time resolution of the absorption spectrometer was determined to be about 120 fs by measuring the ultrafast growth of excited-state absorption (ESA) for tetraphenylprophyrin in benzene or perylene in cyclohexane. The effects of temporal dispersion on the time-resolved spectra were also eliminated by determining the position of the zero delay between the pump and probe pulses by monitoring the growth of ESA of tetraphenylprophyrin in benzene at different wavelengths in the 470−1000 nm region. The temporal profiles recorded using different probe wavelengths were fitted with up to three exponentially decaying or growing components by the iterative deconvolution method using an sech^2-type instrument response function with a fwhm of 120 fs.

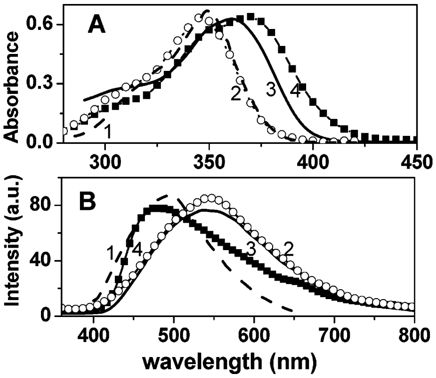

Figure 1. Ground-state absorption (A) and fluorescence (B) spectra of MK in ethyl acetate (1), acetonitrile (2), DMSO (3), and 1-propanol (4).

3. Results

3.1. Steady-State Absorption and Fluorescence. Although the steady-state absorption and fluorescence characteristics of amino-substituted benzophenones, including MK, have been discussed by many authors earlier,[1−10] we need to discuss here a few important features of the steady-state spectroscopic properties of MK for the convenience of the discussion of our results on ultrafast dynamics. Figure 1 shows the steady-state absorption and fluorescence spectra of MK recorded in a few nonaqueous solvents at room temperature. In each of these solvents, the absorption spectrum of MK in the 280−450 nm region is characterized by an intense absorption band, which has been assigned to the $\pi\pi^*$ transition and a shoulder at ca. 310 nm (32 260 cm^{-1}), which has been assigned to the $n\pi^*$ transition.[2] Both the shape and the position of the maximum of the $\pi\pi^*$ absorption band are sensitive to the solvent characteristics. The absorption spectra are nearly identical in ethyl acetate (dielectric constant, $\epsilon = 6.7$) and acetonitrile ($\epsilon = 37.5$), although the polarities of these two aprotic solvents are very different. However, in DMSO ($\epsilon = 47.5$), which is another polar aprotic solvent but known to be a good cation solvator, the band maximum shifts to a longer wavelength and the spectral width (fwhm) of the band also increases significantly. The larger bathochromic shift of the maximum of this absorption band in DMSO compared to those in other aprotic solvents suggests stronger association of the former solvent with the excited state of MK. However, both the bathochromic shift of the maximum and the width of the $\pi\pi^*$ absorption band are much larger in 1-propanol compared to those in aprotic solvents. In addition, in alcoholic solvents the region of maximum absorption of this band appears to have been splited into two bands. One of them appears as a shoulder at the higher energy side of the main band. The broad maximum of the absorption band in alcoholic solutions may arise because of the existence of the intermolecular hydrogen bonded complex and the non-hydrogen-bonded (or uncomplexed) molecules in equilibrium.

The fluorescence spectrum of MK in each of the solvents recorded at room temperature is broad and structureless (Figure 1B). The shape and the maximum of the fluorescence band are sensitive to the characteristics of the solvent, that is, polarity and proticity. Fluorescence maximum undergoes a large bathochromic shift in a more polar aprotic solvent. The Stokes shift is also very large in aprotic solvents and increases with increasing polarity of the solvent. The Stokes shifts are 8451 cm^{-1} in ethyl acetate and 10 637 cm^{-1} in acetonitrile. However, the fluorescence maxima in acetonitrile and DMSO are at the same position and the Stokes shift in DMSO (8640 cm^{-1}) is smaller than that in acetonitrile. The characteristics of the absorption and fluorescence spectra suggest a specific interaction between MK and DMSO in the excited state. The fluorescence maximum is not very sensitive to polarity in the case of alcoholic solvents. The position of the fluorescence maximum (appearing at 482 nm or 20 747 cm^{-1}) is much blue-shifted and the Stokes shift is much smaller (ca. 4597 cm^{-1}) in propanol compared to those in aprotic solvents of even less polarity (e.g., the maximum is at 495 nm or 20 202 cm^{-1} and the Stokes shifts is 8451 cm^{-1} in ethyl acetate). The fluorescence yield is more than one order of magnitude lower in 1-propanol compared to those in acetonitrile and DMSO.[6] However, the yield increases with increasing viscosity (or decrease in proticity) of the alcohols.[6]

Shoute determined the change in dipole moment ($\Delta\mu$) due to photoexcitation of MK as 4.0 and 10.4 D in protic and aprotic solvents, respectively.[6] Hence, he concluded that the fluorescence emission originated from the ICT state in protic solvents, whereas the TICT kind of relaxed S_1 state was responsible for the fluorescence emission of MK in aprotic solvents. These assignments obviously explain the larger Stokes shift in aprotic solvents compared to that in protic solvents of similar polarity. Our ultrafast time-resolved absorption study not only confirms these facts but also provides the microscopic details of the relaxation dynamics of these states (vide infra).

SCHEME 1: Optimized Geometrical Structure of MK in the Ground Electronic State

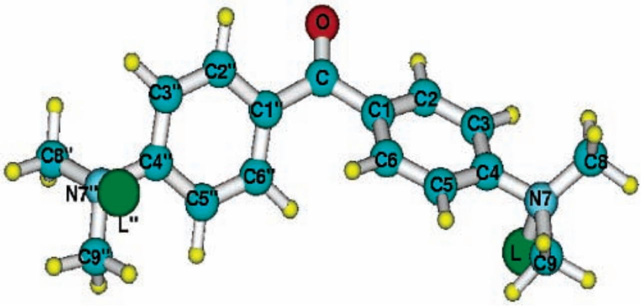

3.2. Theoretical Study. The ground-state structure of MK has been optimized (considering the molecule a C_2 point group) using Hartree−Fock theory with the 6-31G* basis set. The optimized geometrical structure of MK in the ground electronic state is shown in Scheme 1. The selected geometrical parameters, such as bond lengths, bond angles, and dihedral angles of MK are given in Table 1 of the Supporting Information. It is evident from the calculated values of the geometrical parameters that the benzophenone moiety within the MK molecule is not planar; rather, the dihedral angle between the phenyl rings is about 51°. The dipole moment of the ground state is calculated to be 4.1 D. Calculations for the vertical singlet excited state have also been performed using the corresponding ground-state geometry of the molecule. For this purpose, configuration interaction singles (CIS) method was used.[33] The calculated value of the dipole moment of the FC state has been found to be 5.6 D. All of the calculations in this work were done using the GAMESS electronic structure program.[34]

3.3. Spectral and Temporal Characteristics of the Transient Species. We used the transient absorption spectroscopic technique with about 120 fs time resolution to investigate the microscopic details of the relaxation dynamics of the S_1 state of MK in different aprotic and protic solvents of varying polarities and viscosities. For this purpose, 400 nm laser pulses of 50 fs duration have been used for excitation and the temporal absorption profiles have been monitored at different wavelengths in the 470−1000 nm region at 20 nm intervals to construct the time-resolved transient absorption spectra. The MK molecule in nonpolar solvents, such as cyclohexane, is not convenient for the transient absorption study using 400 nm excitation, because, in these solvents, the ground-state absorption spectrum of MK is shifted too far to the blue and the solubility of MK in these solvents is also not high enough to obtain a large enough ground-state absorption for efficient excitation at 400 nm (Figure 1A). Hence, we could study the transient behavior only in relatively more polar solvents, such as ethyl acetate, acetonitrile, and so forth.

The time-resolved transient absorption spectra (a−j) constructed for a few selected time-windows in sub-5 ps time domain following photoexcitation of MK in acetonitrile are presented in Figure 2. Figure 2 also shows the spectrum (spectrum k) recorded at 50 ps after photoexcitation of MK in acetonitrile with 355 nm laser pulses of 35 ps duration.[7] Spectrum a, constructed for 0.15 ps delay time, consists of three major ESA bands in the 470−650, 650−800, and 800−1000 nm regions with maxima at ca. 520, 690, and 930 nm, respectively. In the sub-0.5 ps time-domain, absorbance within the ESA bands in the 470−650 nm and 650−800 nm regions decreases and that in the 800−1000 nm region increases with

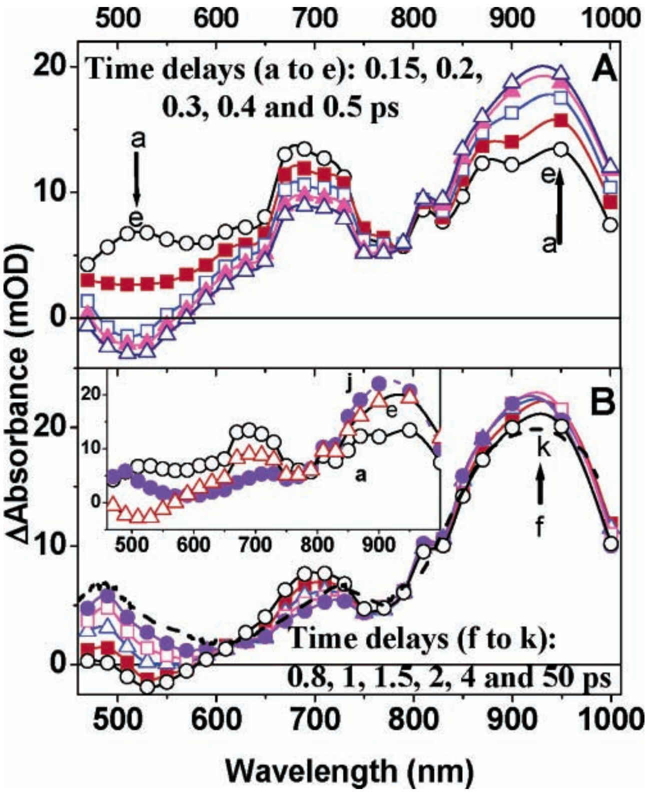

Figure 2. Time-resolved transient absorption spectra constructed for different time delays following the photoexcitation of MK in acetonitrile using 400 nm laser pulses of 50 fs duration. These have been constructed using the temporal profiles monitored in the 470−1000 nm region (a few of which have been presented in Figure 3). The inset shows the transient spectra constructed for 0.15, 0.5, and 4 ps delay times after photoexcitation of MK. They represent the absorption spectra of LE, ICT, and TICT states of MK (vide infra).

increasing delay time (Figure 2A). As a result, spectrum e, constructed for the 0.5 ps delay time shows the presence of a negative absorption band in the 470−570 nm region with maximum at 530 nm and two ESA bands in the 600−1000 nm region. Because the ground-state absorption spectrum of MK in acetonitrile (curve 2 in Figure 1A) shows negligible absorption in the 470−570 nm region, the negative absorption band cannot be assigned to the bleaching of the ground state. However, because the fluorescence spectrum of MK in acetonitrile (curve 2 in Figure 1B) overlaps with this region, the negative absorption band is assigned to the emission from the S_1 state of MK, stimulated by the coherent continuum probe light.

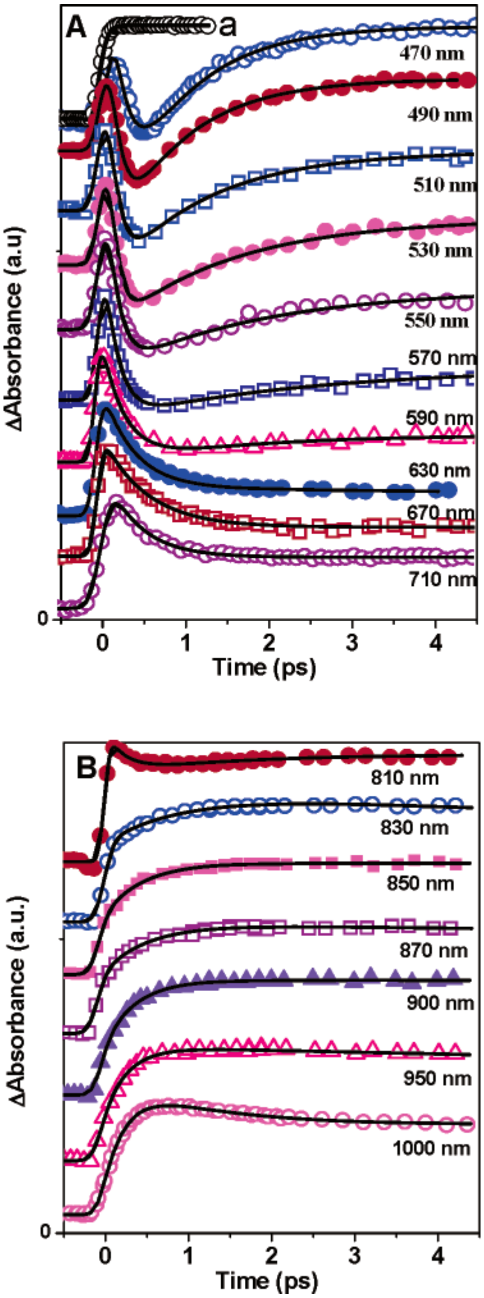

Figure 3. Temporal evolution of transient absorption monitored at different wavelengths following the photoexcitation of MK in acetonitrile using 400 nm laser pulses of 50 fs duration. Solid lines represent the best multiexponential fit functions. Lifetimes of two shorter components (τ_1(d) and/or τ_2(g)) are given in Table 1. The longest decay component (τ_3(d) ≈ 600 ps), which has been fixed during the fitting process, is not given in Table 1. Curve a shows the growth of the S_1 state of perylene in cyclohexane to show the instrument response time (120 fs).

On further increase in delay time beyond 0.5 ps, the "stimulated emission" (SE) band decays and an ESA band in the 470−600 nm region with a maximum at 490 nm develops subsequently within the 5 ps time domain. The ESA band in the 650−800 nm region continues to decay up to about 2 ps, but little further growth of that in the 800−1000 nm region is observed within this time. As a result, the transient absorption spectrum recorded at 4 ps (spectrum j) consists of three ESA bands in the entire 470−1000 nm region (Figure 2B). The main features of this spectrum are very similar to those of spectrum k, which has been recorded at a 50 ps delay time. The transient absorption spectrum, k, was assigned earlier to that of the singlet state of MK.[7] Similarities in the features of spectra j and k suggest that the evolutions of the time-resolved transient absorption spectra observed here in the sub-5 ps time domain following photoexcitation of MK to the S_1 state, which has a much longer lifetime (about 650 ps),[6] represent the relaxation processes taking place in the same state and the same is also complete within 5 ps time. The inset of Figure 2B shows a comparison of the features of the transient spectra recorded immediately after (i.e., spectrum a) and those recorded at 0.5 and 4 ps (spectra e and j, respectively) after photoexcitation of MK to its S_1 state. Spectrum j is assigned to the relaxed S_1 state of MK.

A few typical temporal absorption profiles, which have been recorded using different probe wavelengths following photoexcitation of MK in acetonitrile, are shown in Figure 3. The lifetimes of the different decay (d) and growth (g) components, which were obtained by multiexponential fittings of the temporal

TABLE 1: Time Constants for the Relaxation Dynamics of MK Measured at Different Probe Wavelengths[a]

monitoring wavelength, nm	acetonitrile[b]		DMSO[c]		1-propanol		
	τ_1(d), ps [a_1]	τ_2(g), ps [a_2]	τ_1(d), ps [a_1]	τ_2(g), ps [a_2]	τ_1(d), ps [a_1]	τ_2(g), ps [a_2]	τ_3(d), ps [a_3]
470	0.1 [5]	0.82 [−2.5]	0.11 [2.9]	5.02 [−1.9]	0.1 [3.2]	7.6 [−2.9]	
490	0.11 [8]	0.86 [−3.9]	0.15 [3.5]	6.5 [−2.5]	0.19 [3.2]	11 [−3]	93 [2]
510	0.12 [7.3]	1.4 [−3]	0.18 [4.2]	6.8 [−2.9]	0.3 [3.3]	14.5 [−3]	
530	0.12 [7.2]	1.5 [−2.7]			0.5 [3]	18.3 [−3]	
550	0.13 [5.2]	1.6 [−1.5]	0.22 [3.5]	12.1 [−2.1]	0.5 [3.1]	37 [−3.7]	
570	0.16 [4.3]	1.65 [−0.9]	0.36 [3.1]	12.5 [−1]	0.85 [3.2]	40 [−3.5]	
590	0.28 [2.7]	1.6 [−0.6]			1.6 [3.4]	38 [−6.5]	
610			1.1 [2.5]	12.2 [−1.2]	2.7 [3.7]	38 [−7.1]	
630	0.38 [1.9]	1.5 [−0.1]	1.6 [2]		2.4 [3.5]	36 [−5]	85 [2.8]
650			2.2 [2.2]		2.4 [3.3]	38 [−3.8]	
670	0.5 [3.3]		1.5 [2.6]		2.3 [1.1]	34 [−1.6]	
710	0.45 [2.4]						
730			1.25 [2]		0.9 [1]	24 [−0.5]	long
750			0.85 [1.6]		1.7 [0.4]	7.2 [−0.6]	long
770			1.0 [1.3]	12.0 [−0.1]	0.18 [0.9]	6.0 [−0.4]	90 [−0.1]
810	0.23 [1.6]	1.4 [−0.6]	0.13 [1.2]	10 [−0.6]		4.1 [−1.5]	58.7 [3]
830		0.9 [−1.1]		5.9 [−1]			
850		0.6 [−2]		4.14 [−1]		1.3 [−1.6]	50.6 [3]
870		0.53 [−2.4]		3.2 [−1.5]			
900		0.37 [−3.5]		2.1 [−2]		1.1 [−1.6]	37 [3.1]
950		0.28[d] [−3.6]		1.0[d] [−2.4]		0.73 [−2]	26.7 [4.1]
1000		0.26[d] [−2.2]					

[a] a_1, a_2, and a_3 represent the corresponding relative amplitudes of different components in the multiexponential fitting of the temporal profiles. The negative amplitudes indicate the growing component. [b] τ_3(d) ≈ 600 ps has been fixed in the three exponential fittings of the temporal profiles. [c] τ_3(d) ≈ 850 ps has been fixed in the three exponential fittings of the temporal profiles. [d] The temporal profile is fitted with one growth, τ_2(g), and two decay components (τ'_3(d) and τ_3(d)) (see Figure 4 and the Supporting Information).

profiles using the iterative deconvolution method, are given in Table 1. However, in this table we have not shown the decay lifetimes of those components, which have lifetimes longer than 200 ps, because these lifetimes could not be determined accurately by our spectrometer. The lifetimes of the S_1 state, which are longer than 200 ps, have been determined using the TCSPC technique. Figure 3 reveals that the transient species created by photoexcitation of MK follow multiexponential dynamics and the lifetimes (decay and/or growth) of the different components are dependent on the monitoring wavelength. In Figure 3A, we present the temporal profiles recorded at a few wavelengths within the ESA and/or SE bands in the 470−650 nm and 650−750 nm regions and those recorded in the 800−1000 nm region are presented in Figure 3B. Figure 3A reveals the instrument response-time-limited growth of ESA for each of the temporal profiles recorded in the 470−750 nm region. However, the dynamics of subsequent evolution of the transient absorption signal is dependent on the monitoring wavelength. In the 470−570 nm region, because of strong overlapping of the ESA band with the SE band, which also grows very fast following photoexcitation, ESA undergoes ultrafast decay to reach a negative absorbance value (Figure 2A). However, we observe a further slow growth of ESA to reach a maximum within the 5 ps time domain. The latter has a very long lifetime, τ_3(d). Because of these reasons, the values of the lifetimes obtained by multi-exponential analysis of the temporal profiles were different at different wavelengths in this region and no meaningful assignment of the lifetimes of the different components could be made to specific transient species or processes. The lifetime of the ultrafast decay component, τ_1(d), increases from 0.1 to 0.38 ps and that of the growing component, τ_2(g), which follows the ultrafast decay, also increases from 0.82 ps to about 1.6 ps, as the monitoring wavelength is tuned from 470 to 630 nm. However, within the 630−750 nm band, the dynamics is nearly independent of monitoring wavelength and the temporal profiles show only the presence of the ultrafast decay component, τ_1(d), having a lifetime of 0.45 ± 0.05 ps, to reach a residual absorbance value after 5 ps. The latter indicates the formation of a very long-lived transient species. The temporal profiles have also been recorded at 510 and 550 nm in a longer time domain (up to about 500 ps) (Figure 4). At 550 nm, in addition to a growing ESA component with a growth lifetime of 1.6 ps, we observe another ESA component growing slower than the former beyond 20 ps.

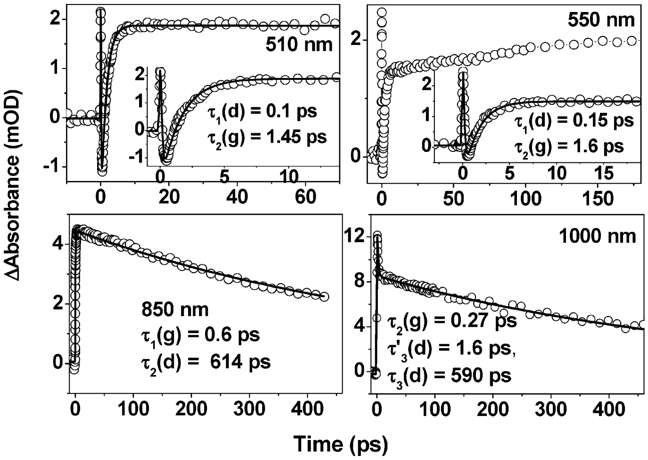

Figure 4. Temporal evolution of transient absorption monitored at four selective wavelengths in a longer (up to 500 ps) time domain following the photoexcitation of MK in acetonitrile using 400 nm laser pulses of 50 fs duration. Solid lines represent the best multiexponential fit functions. The lifetimes are also given in the figure. During the fitting of the temporal curves recorded at 510 and 550 nm, the lifetime of a long decay or growth component (τ_3 > 600 ps) has been fixed. This is not shown in the figure.

Figure 3B reveals that in each of the temporal profiles recorded in the 810−1000 nm region, ESA grows slower than the instrument response time and, here also, the growth lifetime, τ_2(g) (the assignment of the lifetime of this component as τ_2(g) will be clear during the course of discussion), is dependent on the monitoring wavelength. The growth lifetime (τ_2(g) = 0.28

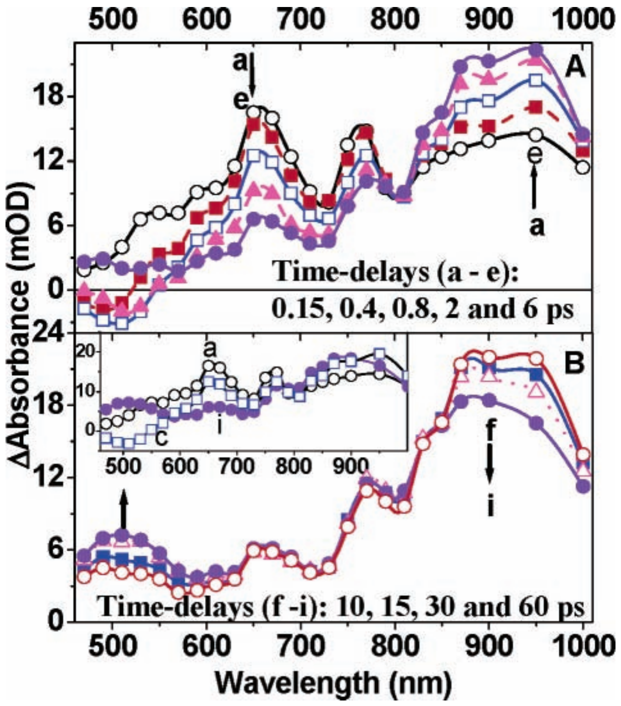

Figure 5. Time-resolved transient absorption spectra constructed for different delay times following the photoexcitation of MK in DMSO using 400 nm laser pulses of 50 fs duration. The inset shows the transient spectra constructed for 0.15, 6, and 60 ps delay times after photoexcitation of MK. They represent the absorption spectra of LE, ICT, and TICT states of MK (vide infra).

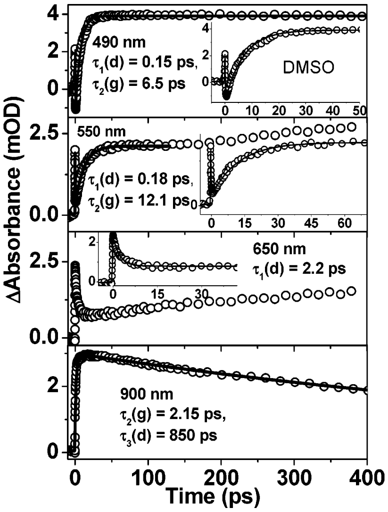

Figure 6. Temporal evolution of transient absorption monitored at four selective wavelengths in longer (up to 400 ps) time domains following the photoexcitation of MK in DMSO using 400 nm laser pulses of 50 fs duration. Solid lines represent the best multiexponential fit functions. The lifetimes are also given in the figure. During the fitting of the temporal curves recorded at 490, 550, and 650 nm, the lifetime of a long decay or growth component (τ_3 > 800 ps) has been fixed. This is not shown in the figure.

ps) is shortest at 1000 nm and increases gradually as the wavelength is tuned toward the higher energy region. The value of τ_2(g) becomes 1.4 ps at 810 nm, which is nearly equal to that (τ_2(g) = 1.6 ps) of ESA monitored in the 550−590 nm region. Because of the overlapping of this near-IR absorption band with the higher energy ESA bands, the presence of another component, which shows instrument response-time-limited growth and an ultrafast decay, is also evident in the temporal profile recorded at 810 nm. In the 800−900 nm region, after attaining the maximum value, ESA decays single exponentially with a long lifetime (τ_3(d) ≈ 600 ± 20 ps) (Figure 4). However, the temporal profiles recorded at 950 and 1000 nm reveal that ESA follows nonexponential decay dynamics because of the presence of a decay component (τ'_3(d)), which decays much faster than τ_3(d) (Figure 4). The value of τ'_3(d) is also dependent on the monitoring wavelength.

The time-resolved spectra of the transient species produced in DMSO are shown in Figure 5. The nature of evolution of the transient spectra recorded following photoexcitation of MK in DMSO is similar to that observed in acetonitrile. However, in the time-resolved transient absorption spectra constructed in DMSO, we observe two new features, which could not be resolved in the case of acetonitrile (compare Figures 2 and 5). In DMSO, we observe a dynamic red shift of the maximum of the SE band in the 470−550 nm region and a change in shape of the ESA band in the 800−1000 nm region.

The characteristics of the temporal profiles recorded in DMSO are very similar to those observed in acetonitrile. Figure 6 presents the temporal profiles recorded up to about 500 ps delay time at a few selective wavelengths. However, the lifetimes of two ultrafast components, τ_1(d) and τ_2(g), which have been obtained from the analyses of the temporal profiles at other wavelengths, are given in Table 1. The decay lifetime, τ_1(d), increases from 0.11 ps to about 1.6 ps, as the probe wavelength is tuned from 470 to 630 nm, because of overlapping of the ESA and SE bands. The value of τ_1(d) remains more or less constant within the ESA band in the 630−700 nm region. τ_1(d) again becomes shorter as the wavelength is tuned toward the near-IR region above 700 nm and this component is not observed at wavelengths beyond 810 nm. The growth lifetime, τ_2(g), also increases from 5.02 to 12 ps as the wavelength is tuned from 470 to 630 nm. In the 550−700 nm region, we also observe another slower growing component. Like in acetonitrile, the temporal profiles recorded at different wavelengths within the 800−1000 nm band show only the ultrafast growth component (presence of the component with lifetime τ_1(d) is absent in this region). The value of τ_2(g) increases gradually as the wavelength is tuned from 1000 to 800 nm. In the 800−850 nm region, ESA, after attaining the maximum absorbance value, decays with a long lifetime of about 850 ps (Figure 6), but beyond 850 nm, we also observe the presence of a faster decaying component, τ'_3(d).

Because of the low solubility of MK in ethyl acetate, temporal profiles could not be recorded at all wavelengths because of the poor signal-to-noise ratio but we managed to record the temporal dynamics of the transient species in this solvent at a few selective wavelengths, which have been presented in Figure 7. In the sub-10 ps time domain, like in other aprotic solvents, we observe the instrument response-time-limited rise of ESA in the 650−710 nm region (Figure 7A). This is followed by the ultrafast decay of ESA with 1.3 ± 0.2 ps lifetime to attain a residual value. However, we observe further growth of ESA in the longer time domain with a growth lifetime of about 100 ps (Figure 7B). However, in the 850−950 nm region, initial growth of ESA is slower than the instrument response-time and the growth lifetime increases from 0.8 ps, measured at 950 nm, to 1.7 ps at 850 nm (Fugure 7A). In longer than a 10 ps time domain, ESA decays with about 90 ps lifetime to leave a small residual absorbance. At 490 nm, we observe the ultrafast decay of ESA, which initially grows with the instrument response time, and then it further grows biexponentially with the lifetimes of 1.7 and 90 ps. In this case, although the transient signal reached

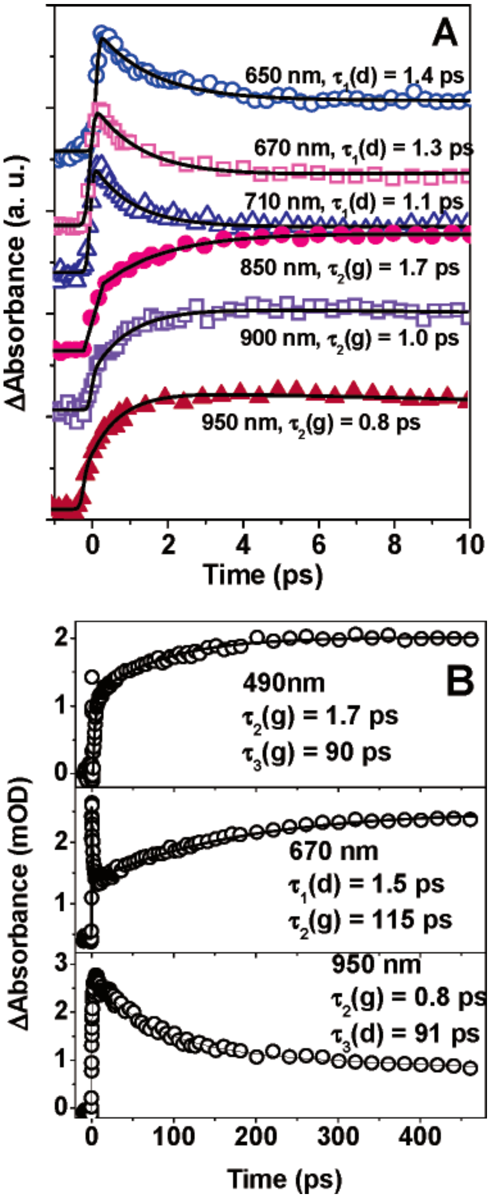

Figure 7. Temporal evolution of transient absorption monitored at a few selective wavelengths in 10 ps (A) and longer (up to 500 ps) (B) time domains following the photoexcitation of MK in ethyl acetate using 400 nm laser pulses of 50 fs duration. Solid lines represent the best multiexponential fit functions. The lifetimes are also given in the figure. During the fitting of the temporal curves, the lifetime of a long decay or growth component ($\tau_3 >$ 200 ps) has been fixed. This is not shown in the figure.

nearly to zero value following the ultrafast decay of ESA, it did not show negative absorption due to stimulated emission.

We also investigated the ultrafast dynamics of the excited state of MK in normal alcohols with the linear hydrocarbon chains of different lengths. The behaviors of the transient species are more or less similar in all of these alcoholic solvents. In Figure 8, we present the time-resolved transient absorption spectra of MK in 1-propanol to show the typical spectral characteristics of the transient species produced due to photolysis of MK in alcohols. Spectrum a, constructed for a 0.15 ps delay time, has three ESA bands in the 510−1000 nm region and a SE band in the 470−510 nm region. One of the ESA bands has a maximum at ca. 630 nm and a shoulder at ca. 550 nm, and the other two have maxima at ca. 710 and 970 nm, respectively. In the sub-6 ps time-domain, the ESA band in the 600−750 nm region decays accompanied by the concomitant growth of another ESA band in the 800−1000 nm region. As a result, we observe a temporary isobestic point at ca. 750 nm. The SE band also decays accompanied by a dynamic red shift of the maximum, which appears at <470 nm at 0.2 ps but shifts to 530 nm after about 10 ps delay time. With further increase in the delay time beyond 6 ps, the ESA band in the 800−1000 nm region starts decaying and the decay is nearly complete within about 150 ps. However, we observe the growth of the ESA band in the 470−670 nm region between the 6 and 50 ps time domain, before it starts decaying with further increase in delay time. However, unlike the ESA band in the 800−1000 nm region, the decay of the ESA bands in the 470−800 nm region is not complete within 150 ps because of the longer lifetime of the transient.

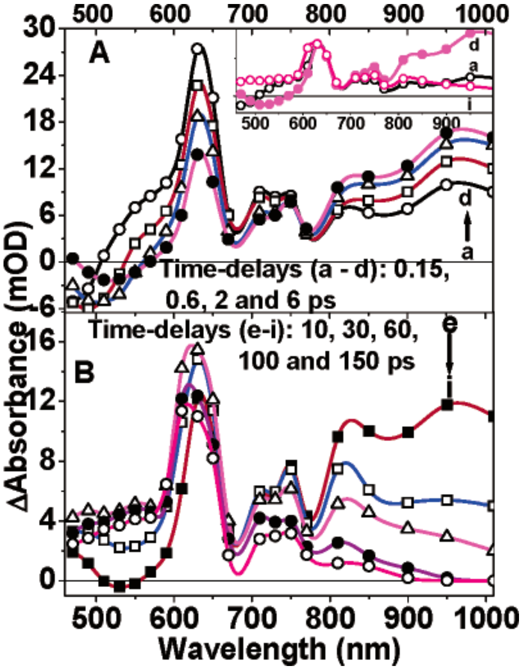

Figure 8. Time-resolved transient absorption spectra constructed for different time delays following photoexcitation of MK in 1-propanol using 400 nm laser pulses of 50 fs duration. The inset shows the transient spectra constructed for 0.15, 6, and 150 ps delay times after the photoexcitation of MK. They represent the absorption spectra of LE, ICT, and TICT states of MK (vide infra).

Figure 9 presents the temporal profiles recorded at different wavelengths up to about 150 ps delay time. They corroborate the facts described in the previous paragraph. Figure 9A reveals that, immediately after the laser pulse, SE appears in the 470−510 nm region (unlike in aprotic solvents, instrument-response-time-limited growth of ESA is not observed here). The growth lifetime of SE (which has also been represented as τ_1(d) in Table 1 because of the positive coefficient of the term related to this component in the fitting function) is wavelength-dependent and becomes longer as the wavelength is tuned from 470 to 510 nm. However, in the temporal profiles recorded at the wavelengths beyond 530 nm, ESA appears immediately after the laser pulse and its decay lifetime, τ_1(d), like in aprotic solvents, also increases as the wavelength is tuned from 530 to 610 nm. In addition, the subsequent growth of ESA also becomes slower as the wavelength is tuned from 470 to 610 nm and the value of the growth lifetime, τ_2(g), becomes 40 ps at 570 nm. Both τ_1(d) (=2.5 ± 0.2 ps) and τ_2(g) (=37 ± 3 ps) remain more or less constant in the 600−700 nm region. Figure 9B and Table 1 reveal that, in this solvent also, the lifetimes of all three components, namely, τ_1(d), τ_2(g), and τ_3(d), which are associated with the temporal evolution of the ESA band in the 730−1000

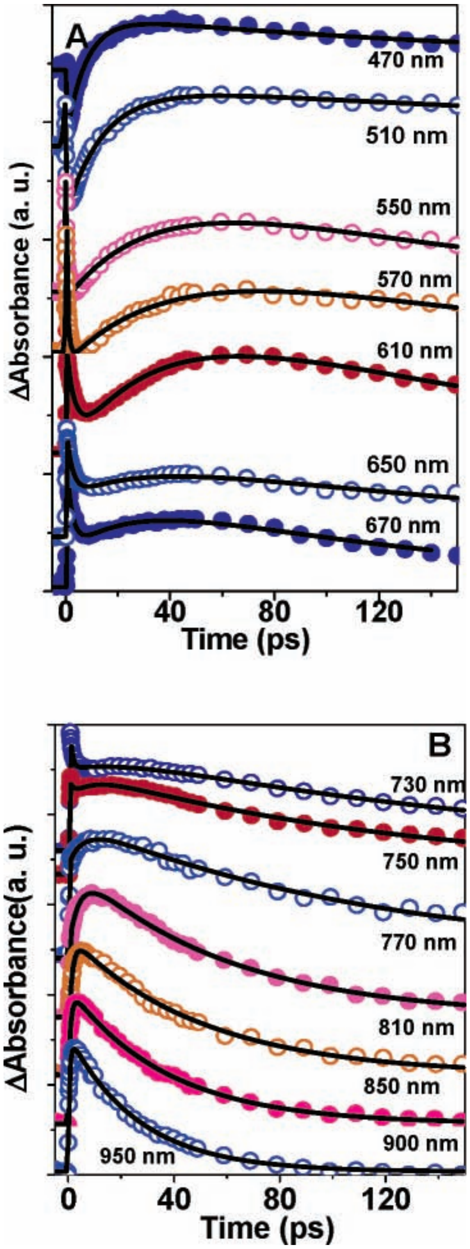

Figure 9. Temporal evolution of transient absorption monitored at different wavelengths following photoexcitation of MK in 1-propanol using 400 nm laser pulses of 50 fs duration. Solid lines represent the best multiexponential fit functions. The lifetimes of components τ_1(d), τ_2(g), and τ_3(d) are given in Table 1. In some cases, τ_3(d) is longer than 200 ps and could not be determined accurately and hence not given in Table 1.

nm region, are strongly dependent on the monitoring wavelength. In the 770−1000 nm region, the component with lifetime τ_1(d) is absent but both τ_2(g) and τ_3(d) increase as the wavelength is tuned from 1000 to 750 nm.

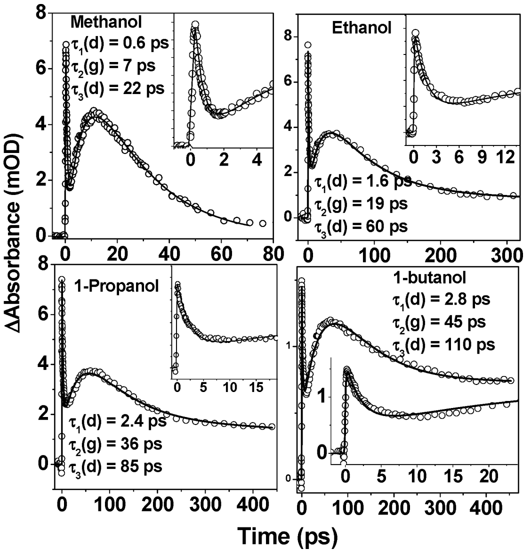

Figure 10. Temporal evolution of transient absorption monitored at 630 nm following photoexcitation of MK in four alcoholic solvents using 400 nm laser pulses of 50 fs duration. Solid lines represent the best quadric exponential fit functions. The lifetimes are also given in the figure. During the fitting of the temporal curves, the lifetime of the long decay component (τ_4(d) > 500 ps) has been fixed. This is not shown in the figure.

Figure 10 presents the temporal behaviors of the transient species recorded at 630 nm (see the Supporting Information for those recorded at 490 nm) up to about 450 ps delay time in 1-propanol as well as in methanol, ethanol, and 1-butanol. Although the temporal profiles have been recorded in methanol and ethanol at other wavelengths as well (see the Supporting Information), we present the results obtained by analyzing only those recorded at 630 nm because our analyses of the temporal profiles recorded in 1-propanol show that information regarding the formation and decay lifetimes of the transient species involved in the relaxation dynamics of the S_1 state of MK can be measured accurately at this wavelength avoiding interference from the stimulated emission (Figure 9). Each of these temporal profiles has been fitted by a quadric exponential function to obtain the values of τ_1(d), τ_2(g), and τ_3(d). The fourth component is a small long-lived residual absorption. The characteristics of the temporal curves presented in this figure clearly reveal the similarities in the dynamics in the alcoholic solvents. We could not study the dynamics in alcoholic solvents with the alkyl chain longer than that of 1-butanol because of the longer lifetime of the transient species, which could not be measured using our femtosecond spectrometer, as well as the higher yield of the triplet state masking the true features of the relaxation dynamics of the S_1 state.

4. Discussion

4.1. Origin of Different Lifetime Components. Our time-resolved absorption measurements reveal that the features of the relaxation dynamics of the S_1 state of MK are very similar to those reported by Glasbeek and co-workers, who used the ultrafast fluorescence spectroscopic technique.[1] The excited-state dynamics of MK is ultrafast, multiexponential, and the lifetimes of the different components are dependent on the probe wavelength as well as on the viscosity of the medium. Apparently, the wavelength-dependent dynamics of the transient species observed in the present case seems to be very complicated. However, a careful examination of the lifetimes of the different components associated with the multiexponential temporal profiles recorded at different wavelengths ranging from 470 to 1000 nm in each of the solvents reveals that the dynamics of the S_1 state relaxation processes of MK can be explained by invoking the concept of twisting of the dimethylanilino groups with respect to the central carbonyl group leading to conversion of the FC or LE state to the TICT state, as suggested by Glassbeek and co-workers as well as by Shoute.[1,6] Twisting can be shown to be the major process controlling the relaxation dynamics of the S_1 state. We present below a detailed discussion of our results obtained in different kinds of solvents in the light of the twisting process, taking place in the S_1 state of MK.

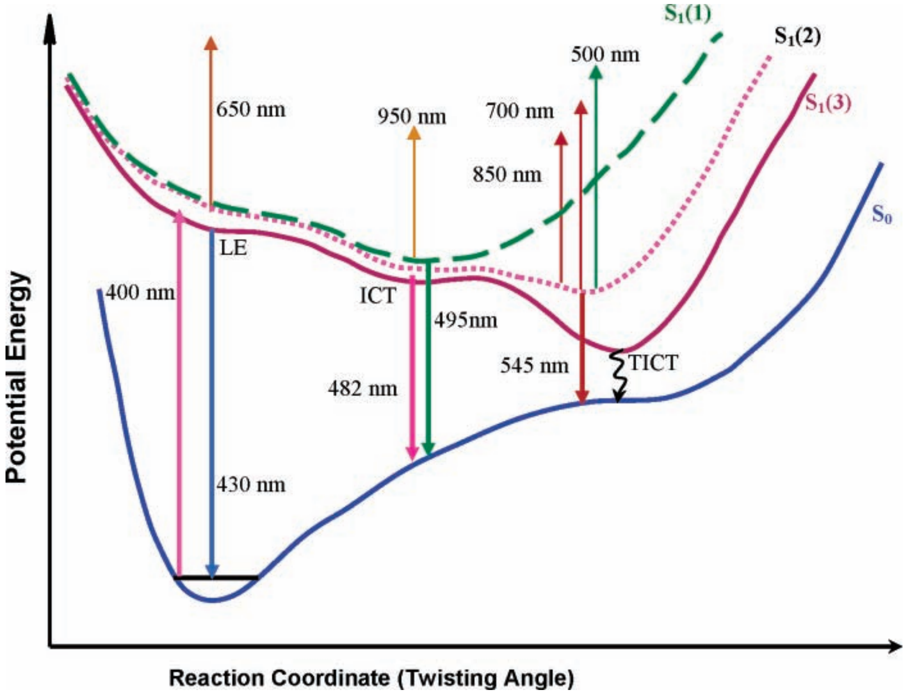

Figure 11. Oversimplified two-dimensional potential energy surface (PES) diagram for the relaxation dynamics of the S_1 state of MK. The shape of the PES for the S_1 state is solvent-dependent. Curves $S_1(1)$, $S_1(2)$, and $S_1(3)$ represent the PES of the S_1 state in nonpolar aprotic, polar aprotic, and polar protic solvents, respectively. The LE to TICT involves two kinds of diffusive twisting motions: ultrafast antitwisting motion of dimethylanilino group to form the ICT state and twisting of the dimethylamino group with respect to the phenyl group to form the TICT state. Different possible $S_n \leftarrow S_1$ transitions observed in the present study have been indicated by vertical upward arrows and the fluorescence emission from the LE, ICT, and TICT states are shown as vertical downward arrows. The curved arrow indicates very efficient nonradiative relaxation from the TICT state to the ground state in alcoholic solvents.

The ground-state absorption spectra of MK presented in Figure 1A suggest that 400 nm light excites the molecules of MK near the lowest energy vibrational level of the lowest excited singlet (S_1) state. Hence, the possibility of the contribution of the vibrational cooling process to the temporal dynamics of the transient species can be excluded safely. The wavelength dependence of the temporal profiles recorded in the 470−650 nm region is a result of overlapping of the ESA and the SE bands of more than one kind of transient species formed following photoexcitation of MK in solution. We have not made any attempt to reconstruct the actual shapes of the ESA and SE bands in the 470−650 nm region because of the lack of knowledge of the absorption coefficient for $S_n \leftarrow S_1$ transitions and the cross sections of SE occurring from the S_1 state at different wavelengths. Without having quantitative knowledge of these two parameters, correction of the transient spectra might have led to some meaningless interpretation. However, the wavelength dependence of the temporal profiles recorded in the 650−1000 nm region, which is free from the overlapping effect of the SE band, clearly reveals the dynamics of the relaxation process happening along the twisting coordinate of the potential energy surface (PES).

The ultrafast and nonexponential dynamics of the S_1 state of a few other TICT kinds of molecules, such as bacteriorhodopsin, photoactive yellow protein, cyanine dyes such as LDS-821, auramine, and dimethylaminobenzophenone has been explained following a three-state model.[15,21,25a,35−37] In this model, immediately after photoexcitation, the system decays very rapidly out of the FC region into a nearly flat region of the PES to form the reaction region, called the LE state. In this region, there is an anticrossing with another excited electronic state, called the TICT state, which is separated from the LE state by a small or no barrier. The LE → TICT conversion process, which involves the twisting of the phenyl or substituted-phenyl groups, is accompanied by further charge transfer, and, hence, the TICT state should have a larger dipole moment than that of the LE state. Fluorescence is assumed to take place predominantly when the molecule is in the reaction region.[37] The wavelength-dependent nonexponential dynamics of the excited state is a very regular feature in this kind of molecular system and may arise for several reasons. The most common reason is the motion of the excited state along the steep slope of the barrierless PES because of the conformational relaxation process. Inhomogeneous broadening due to ill-defined surroundings may also be held responsible for the nonexponential dynamics. Because the LE → TICT conversion process is accompanied by separation of charge in the molecule (i.e., creation of larger dipole), solvation is also expected to play a significant role in the relaxation process of the S_1 state.[38]

In acetonitrile and DMSO, the instrument-response-time-limited rise and ultrafast decay of the transient species, which have the lifetimes, τ_1(d), of 0.45 ± 0.1 ps and 1.6 ± 0.2 ps, respectively, measured in the 630−750 nm region, can be assigned to that of the LE state. Decay of the LE state results in the growth of the TICT state, which is observed by monitoring ESA in the 800−1000 nm region. However, the growth lifetime of the TICT state, τ_2(g), is wavelength-dependent and τ_2(g) increases as the wavelength is tuned from 1000 to 800 nm. This can possibly be explained by the fact that the probe lights of different wavelengths monitor the transient species, which have different conformation with different geometries corresponding to different regions of the PES (Figure 11). The probe light of shorter wavelength or higher energy monitors the region of the PES, which corresponds to the minimum potential energy of the TICT state (Figure 11). Hence, the growth lifetime, τ_2(g), measured at the extreme blue edge of the ESA band, which is the characteristic of the TICT state (curve j in Figure 2 and curve i in Figure 5), can be assigned to the lifetime of formation

TABLE 2: Decay Lifetimes of the LE, ICT, and TICT States

solvent (ϵ; η, mN·s·m^{-2}; $\langle\tau\rangle_{solv}$, ps)	lifetime of the LE state (τ_{LE}), ps	lifetime of the ICT state, (τ_{ICT}), ps	lifetime of the TICT state, (τ_{TICT}), ps
cyclohexane (0.98; 2.02; −)		6.7	
benzene (2.27; 0.60; 2.1)		2.5	
ethyl acetate (6.02; 0.43; 2.6)	1.3	100	
acetonitrile (37.5; 0.34; 0.26)	0.45	1.6	600[a]
DMSO (46.6; 2.0; 1.8)	1.5	12	850[a]
methanol (32.7; 0.55; 5)	0.6	7	23
ethanol (24.55; 1.08; 16)	1.6	19	70
propanol (19.9; 1.94; 26)	2.4	36	90
butanol (17.5; 2.57; 63)	3.0	45	110
pentanol (13.9; 3.6; 103)			130[a]
octanol (10.3; 6.13; −)			210[a]
decanol (13.8; 11; 259)			280[a]

[a] Fluorescence lifetimes.

of this state. These lifetimes are 1.4 and 12 ps in acetonitrile and DMSO, respectively, measured at 810 nm. These are much longer than the decay lifetimes of the LE state in the corresponding solvents. This suggests that after crossing the reaction region of the PES corresponding to the minimum potential energy of the LE state, the system continues to evolve along the PES representing the twisting motion, for longer time to reach the minimum energy region for the twisted S_1 state. Hence, it is important to address the question whether the PES between the reaction region for the LE state and that for the TICT state is barrierless or is associated with another local minimum or reaction region between these two.

We mentioned earlier that both the growth and decay lifetimes of the LE and TICT states measured in the 470−600 nm region are wavelength-dependent because of overlapping of the SE and ESA bands. The largest value of τ_2(g) (i.e., 1.5 ± 0.1 ps and 12.0 ± 0.5 ps in acetonitrile and DMSO, respectively), which has been measured at wavelengths in the 550−600 nm region, are nearly equal to those measured at 810 or 770 nm in the corresponding solvents. Hence, they obviously represent the formation lifetimes of the TICT state. The decay lifetimes of this state, which have been measured at different wavelengths in the 810−850 nm region, are very long in both solvents and have been confirmed by measuring the fluorescence lifetime ($\tau_F \approx 600$ and 850 ps in acetonitrile and DMSO, respectively, Figures 4 and 6 and Table 2). However, the presence of another shorter-lived decay component, τ'_3(d), in the temporal profiles recorded at 950 and 1000 nm (Figure 4) indicates the involvement of an intermediate state in the process of conversion of the LE state to the TICT state.

Following the above arguments, the transient spectrum recorded immediately after the exciting laser pulse, that is, recorded at 0.15 ps (curve a in Figures 2 and 5), can be assigned to the LE state and the transient absorption spectrum recorded at 4 ps in acetonitrile (curve j in Figure 2) or 60 ps in DMSO (curve i in Figure 5), (these delay times are longer than the five half-lives of the growth lifetime of the TICT state in the corresponding solvent) can be assigned to the TICT state. The transient spectrum of the LE state consists of three ESA bands with maxima at 510 (550), 650 (670), and 950 (950) nm in acetonitrile (DMSO), and that of the TICT state has three distinct absorption bands with maxima at ca. 490 (500), 730 (670), and 900 (850) nm in acetonitrile (DMSO). In DMSO, there is an extra band with maxima at 750 nm for both the LE and TICT states.

Fluorescence emission takes place predominantly when the molecule is in the reaction region, which is represented by a local minimum on the PES. Evolution of the time-resolved spectra in the sub-0.5 ps time-domain in acetonitrile (Figure 2A) and in the sub-6 ps time-domain in DMSO (Figure 5A) reveal the growth of SE in the 470−550 nm region concomitant with the decay of the LE state. This confirms the presence of another reaction region or local minimum on the PES, between those corresponding to the LE and TICT states. This state will be designated hereafter as the ICT state (vide infra). This interpretation is further corroborated by the lack of precursor−sater relationship between the LE and TICT states. The transient spectra of the ICT state in acetonitrile are presented in the inset of Figure 2B and that in DMSO in the inset of Figure 5B. The lifetimes of the LE, ICT, and TICT states in different solvents are given in Table 2.

In the case of ethyl acetate, which is an aprotic solvent but with lower polarity than that of acetonitrile or DMSO, the temporal profiles recorded at different wavelengths in the sub-10 ps time-domain reveal the involvement of mainly two kinds of transient species, which have a precursor−sater relationship. The LE or FC state formed following photoexcitation of MK, decays with lifetime, τ_1(d), of 1.3 ± 0.2 ps, which has been measured at wavelengths in the 650−750 nm region (Figure 6A). The growth lifetime of the relaxed state ($\tau_2(g) = 1.3 \pm 0.5$), which has been measured in the 800−950 nm region, is nearly equal to that of the decay of the LE state. The large variation of the values of τ_2(g) in the 800−950 nm region is possibly justifiable considering the arguments provided earlier that different probe wavelengths monitor the different regions of the PES. The precursor−sater relationship between the LE and the relaxed state clearly suggests that, in this solvent, only the conversion from the LE to the ICT state is observed. Possibly, further relaxation of the ICT state to the TICT state is not an energetically favorable process in the solvents of lower polarity. At a longer time domain (beyond 10 ps), while the decay of ESA with the lifetime, τ_3(d), of about 100 ± 10 ps, monitored in the 800−950 nm region represents the disappearance of the ICT state, the growth of transient absorption in the 490−700 nm region with the growth lifetime, τ_3(g), having nearly the same value, represents the formation of the triplet state.

In alcoholic solvents, the dynamics is very similar to that in polar aprotic solvents. Following the arguments presented in the previous paragraphs, the time-resolved spectra recorded at 0.15, 6, and 60 ps can be assigned to the LE, ICT, and TICT states, respectively, produced in 1-propanol (inset of Figure 8A). In alcoholic solvents, the lifetime of the TICT state, τ_3(d), is much shorter compared to those in aprotic solvents because of the strong hydrogen-bonding interaction between the highly polar TICT state and the alcoholic solvents. The lifetime is as short as 23 ps in methanol compared to 600 and 850 ps in acetonitrile and DMSO, respectively. However, the lifetime of

SCHEME 2: Twisting Dynamics of MK in the S_1 State

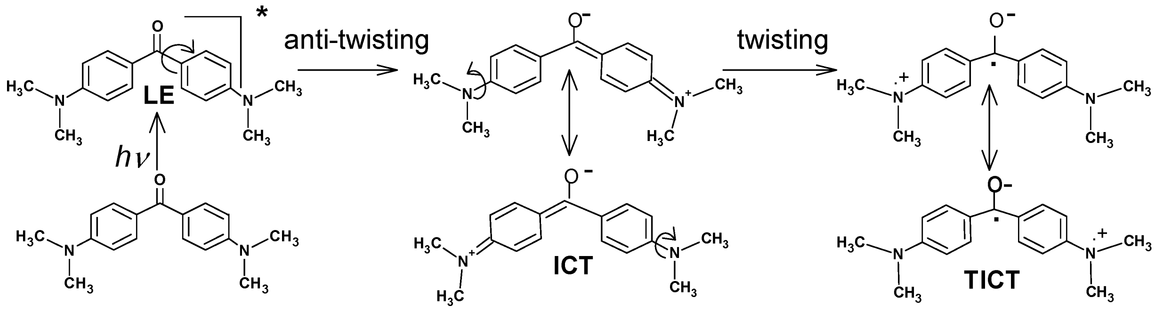

the TICT state increases from methanol to 1-decanol (Table 2 and vide infra). Following the decay of the TICT state, a long-lived residual absorption survives because of formation of the triplet state formed via an intersystem crossing process. The relative amplitude of the residual absorption increases with increasing length of the alkane chain of the alcohol. The triplet yield increases from methanol to 1-butanol. To obtain a more accurate value of the lifetime of the S_1 state by avoiding the interference due to triplet absorption, we also recorded the temporal profiles at 490 nm (Supporting Information), at which wavelength the absorption coefficient of triplet absorption is relatively smaller and obtain the similar values of τ_2(g) and τ_3(d).

4.2. Twisting Dynamics. The discussion in the previous section revealed that the relaxation dynamics of the S_1 state of MK in polar solvents can be described following a kinetic model, which considers the involvement of three kinds of excited states. The same model was adopted to explain the relaxation dynamics of the excited states of the donor−acceptor biphenyl, stilbene, and other polyene derivatives as well as the TPM dyes.[18,39−45] The relaxation process of the S_1 state of MK has been presented schematically in Scheme 2. Theoretical optimization of the ground-state geometry of MK has revealed that in this state the MK molecule has a geometry that is far from planar because of steric interaction between the phenyl rings. The planes of the phenyl rings are rather at a dihedral angle of about 51° with each other. As a result, the extent of charge transfer from the dimethylanilino groups to the carbonyl group is rather low and, hence, the dipole moment of the molecule in the ground state is only 4.1 D. However, following photoexcitation, the MK molecule relaxes very quickly to bring back the pretwisted molecule to the planar geometry by the anti-twisting motion of the dimethylanilino groups attached to the carbonyl group, to form the ICT state. The ICT state is actually a resonance-type state with high mesomeric interaction and nearly planar geometry.[18,39−45] Studies on TPM dyes and many other systems containing dimethylanilino groups attached to a central carbon atom have established the fact that the anti-twisting motion of the dimethylanilino groups is extraordinarily fast and the planarity of the molecule is achieved within a few picoseconds.[22,23,42] In highly polar solvents, the MK undergoes another twisting motion in which the dimethylamino group is completely twisted (to about 90°) with respect to the phenyl ring to which it is attached, producing the TICT state. Among the numerous donor−acceptor molecules with a dimethylanilino or aliphatic amino group as the donor studied and reported in the literature, in the TICT states of most of these molecules, the positive charge remains localized on the amino nitrogen atom.[18,46,47] However, in a few of the cases, the positive charge is distributed over the whole dimethylanilino radical cation.[43,44,48] In the present case, because we could not perform the calculation for the charge distribution in the excited state, considering the results reported earlier on the studies of p-carbonyl derivatives of *N*,*N*-dimethylaniline, we suggest the localization of positive charge on the dimethylamino group.[46,47] The large dipole moment (∼14.5 D) of the TICT state suggests that near-complete transfer of an electron from the dimethylamino group to the carbonyl oxygen and the TICT state may be considered as a pure ET state.[18,46,47] As conclusive evidence in favor of the pure ET state, the transient spectrum assigned to the TICT state should be the sum of the spectra of the *N*,*N*-dimethylamine cation radical ($DMA^{\bullet+}$) and the anion radical of 4-*N*,*N*-dimethylamino benzophenone ($DMABP^{\bullet-}$).[39,47,49] The spectrum of $DMA^{\bullet+}$ is expected to occur in the UV region, which is inaccessible by our experimental setup.[50] Recently, we have characterized the anion radicals of differently substituted aminobenzophenones, including MK, using an electron pulse radiolysis technique.[51] The absorption spectrum of each of the dimethylamino-substituted benzophenone anion radicals shows two major absorption bands in the 450−750 nm region. However, the maximum position of these bands are dependent on the nature of substitution (see the Supporting Information).[50,51] The absorption spectrum of the TICT state in acetonitrile or DMSO also has two absorption bands in the 470−600 and 600−750 nm regions with maxima at ca. 510 and 670 nm, respectively, and the spectrum of the TICT state in this region has been seen to be very similar to the anion radical of MK. Considering the fact that in the TICT state the cation and anion radicals have been the part of the same molecule, rather they are generated as separate entities, the presence of the absorption bands at ∼500 and 670 nm can be taken as strong evidence for the pure ET character of the TICT state.

The above scheme of the relaxation dynamics of the S_1 state of MK is well supported by the steady-state fluorescence spectroscopic data reported by earlier authors as well as presented in this paper. The fluorescence spectrum of MK in ethanol glass recorded following photoexcitation at 400 nm was reported to have a maximum at ca. 435 nm.[4,5b] Because the molecular motion is nearly frozen in rigid matrixes at 77 K, the emission may be considered to be taking place from the FC or LE state. This emission spectrum is much more blue-shifted compared to those recorded in different solvents at room temperature (Figure 1). The room-temperature emission spectra are broad and structureless and the maxima arise at ca. 482, 495, and 543 nm in 1-propanol, ethyl acetate, and acetonitrile, respectively. Hence, they cannot be assigned to the LE state. We assign the emission maximum appearing at 482 nm in 1-propanol to the ICT state and at 543 nm in acetonitrile and DMSO to the TICT state This assignment is in agreement with Shoute.[6] However, we observe the long tail extending up to 800 nm in the fluorescence spectrum recorded in 1-propanol, indicating a weak emission from the TICT state. Very efficient nonradiative coupling of the TICT state with the ground state because of the very small energy gap between these two states in the TICT region causes the latter to be weakly fluorescent or nearly nonfluorescent. However, the large width of the fluorescence spectrum in acetonitrile or DMSO has arisen because of overlapping emission from both the ICT and TICT states as well as the nearly flat nature of the PES in the reaction regions of the ICT and TICT states. The emission maximum in ethyl acetate arises because of emission from the ICT state.

A comparison of the nature of evolution of the time-resolved spectra and the values of the decay lifetimes of the LE state, τ_1(d), in aprotic and protic solvents does not reveal any significant difference in the dynamics of conversion of the LE to the ICT state in these two kinds of solvents. However, it is important to note that, unlike that in aprotic solvents, in alcoholic solvents, SE appears in the 470−510 nm region immediately after the laser pulse with the instrument-response-time-limited rise time. This suggests that, in aprotic solvents, the slope of the PES in the region for the LE state is larger compared to that in protic solvents and the molecule passes through this region quickly without emitting. However, in alcoholic solvents, because of the flatness of the PES in this region, the molecule remains in this region for a longer time to emit from this state. Another important difference noticed in the relaxation dynamics in these two kinds of solvents is that the growth lifetime of the TICT state, τ_2(g), is about three times longer in 1-propanol (η = 1.94 cP) than that in DMSO (η = 2.0 cP). These differences may be ascribed to the hydrogen-bonding effect in alcoholic solvents. In many other cases reported earlier, the barrier height for the conversion of the LE to the TICT state is expected to be higher in alcohols because of the hydrogen-bonding interaction between the dimethylamino group of MK and the alcoholic hydroxyl group.[18] The hydrogen bond withdraws an electron from the electron-donating dimethylamino part and thereby opposes ET to the C=O part. For charge transfer to occur, the hydrogen bond must be broken. This increases the barrier or reduces the steepness of the PES in the reaction regions.

4.3. Viscosity Dependence of the Lifetime Components. The lifetimes of all three states, namely, LE, ICT, and TICT, involved in the relaxation dynamics of the S_1 state of MK are listed in Table 2. The lifetime of the TICT state, represented by τ_{TICT}, does not follow any trend in viscosity dependence because of the obvious reason that the decay process does not involve crossing of the barrier but only radiative and/or nonradiative transition to the S_0 state. However, τ_{LE} as well as τ_{ICT} show a regular increase with increase in viscosity of all kinds of solvents. This suggests that the LE → ICT and ICT → TICT conversion processes must be accompanied by some kind of intramolecular motions, which must be associated with the crossing of a barrier of finite height on the PES.[11,15, 21−23,27]

Numerous theoretical and experimental studies of isomerization or conformational relaxation dynamics have led to the formulation of an empirical power law expression, which fits all of the data for the rate constants of isomerization or conformational changes and can be written in the form[52,53]

$$k_{\text{iso}} = \left(\frac{B}{\eta^{\alpha}}\right) \exp\left(-\frac{E_{\text{act}}}{RT}\right) \qquad (1)$$

The first term (i.e., B/η^{α}, where B is a constant, and $0 \le \alpha \le 1$) is a universal function of viscosity and represents the friction or the dynamical effects exerted by the surrounding solvent or medium opposing the motion of the parts of the molecule involved in the conformational relaxation process. The second term, $\exp(-E_{\text{act}}/RT)$, represents the barrier or static effects represented in the form of activation energy for the conformational relaxation process. At a particular temperature and in a particular class of solvents, in which E_{act} remains more or less unchanged, the exponential term may be considered as a constant factor and hence eq 1 may be written as

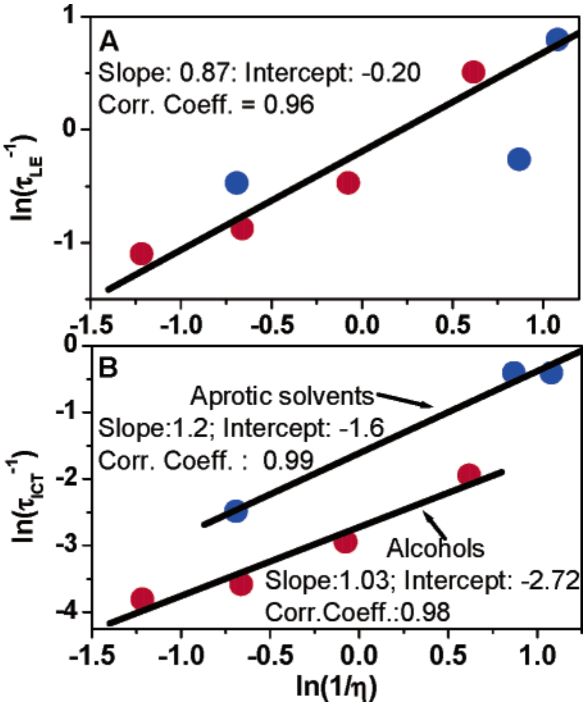

Figure 12. Plots of $\ln(\tau_{\text{LE}}^{-1})$ and $\ln(\tau_{\text{ICT}}^{-1})$ vs $\ln(1/\eta)$ following eq 2.

$$\ln(k_{\text{iso}}) = \alpha \ln\left(\frac{1}{\eta}\right) + C \qquad (2)$$

A plot of $\ln(k_{\text{iso}})$ versus $\ln(1/\eta)$ should be a straight line with a positive slope having magnitude equal to α and the intercept is equal to the constant, $C = \ln(B) - E_{\text{act}}/RT$. Figure 12 represents such plots revealing the logarithmic relationship between the rates of the conversion processes and the viscosities of the solvents. In Figure 12A, the $\ln(1/\tau_{\text{LE}})$ versus $\ln(1/\eta)$ plot shows a similar kind of linear dependence in both kinds of solvents, aprotic and protic. However, the linear dependence of $\ln(1/\tau_{\text{ICT}})$ on $\ln(1/\eta)$ is different in aprotic and protic solvents, possibly because the nature and strength of the interaction between the solvent and the polar ICT state are different in these two classes of solvents. In alcoholic solvents, the ICT state is expected to have a stronger interaction between the polar ICT state of the molecule and the solvent via an intermolecular hydrogen bond.

One of the most important findings from the studies on conformational relaxation processes reported earlier is that, in the case of larger barrier height for photoisomerization or conformational relaxation processes, the rate for the same has a less strong dependence on viscosity of the solvents as measured by the value of α.[52] Hence, the smaller value of α indicates a larger barrier height for the isomerization reaction. As the barrier gets smaller, the barrier-crossing process is controlled by the dynamical interactions influenced by intramolecular motions via intermolecular exchange of energy and momentum. In this case, the bulk viscosity should govern the momentum transfer and, hence, the barrier-crossing dynamics.[54] For both conversion processes, namely, LE → ICT and ICT → TICT, α is nearly equal to unity for both classes of solvents. This suggests that the conformational relaxation processes associated with these lifetimes are nearly barrierless. The conformational relaxation process via diffusive rotation of the *N*,*N*-dimethylanilino groups has been seen to be nearly barrierless (or quasi-barrierless) in many classes of molecules.[15,22,23,25a]

4.4. Twisting versus Solvation Dynamics. A large difference in the dipole moment ($\Delta\mu$ = 10.4 D) between those of the intramolecular charge transfer (ICT or TICT) state and the ground state suggests that solvation dynamics is expected to make a significant contribution to the relaxation dynamics of MK in polar solvents. From the femtosecond fluorescence up-conversion study, Glasbeek and co-workers concluded that both the solvation and phenyl twisting processes were equally important for the relaxation dynamics of the S_1 state of MK.[1] They also inferred that the solvation was very fast in aprotic solvents, but in aprotic solvents slow solvent limit applied. In these solvents, the reaction started by solvation but very soon twisting took over and virtually determined the dynamics of the reaction. However, the results of the present transient absorption study reveals more clearly only the role of the twisting dynamics in the excited relaxation process of MK. Hence, we need to discuss the role of solvation in the same process, considering the results of both the fluorescence study reported by Glasbeek and co-workers as well as the present transient absorption study. A few among other important observations made by Glasbeek and co-workers are that the characteristic time constant of the dynamic Stokes shift determined from the time-resolved fluorescence spectra in each solvent is much faster than the average solvation time and the dynamic Stokes-shifted time-resolved fluorescence spectra are accompanied by the concomitant decay of the integrated fluorescence intensity. Both of these properties of the time-resolved fluorescence spectra are not expected to be observed in a case in which solvation of the polar excited state is the only process responsible for the dynamic Stokes shift.[12] To explain this kind of behavior of the dynamics Stokes shift observed for MK, we have predicted the interplay of both the solvation and twisting processes.

Table 2 shows that the decay lifetimes of the LE state, τ_{LE}, measured in aprotic solvents are nearly equal to or a little shorter than the average solvation time of the solvents $\langle\tau_{solv}\rangle$ and it may be considered that the LE → TICT conversion process is controlled by solvation dynamics. However, the measured values of τ_{LE} in protic solvents are much shorter than $\langle\tau_{solv}\rangle$. We observe the dynamic Stokes shift of the SE band in DMSO and 1-propanol, but because of the very weak nature of the SE band and the strong overlapping of the SE band with the ESA band, the time correlation function of the dynamic Stokes shift of the maximum of the SE band could not be determined. However, the time scale ($<$10 ps), at which the dynamic Stokes shift of the SE band occurs in 1-propanol is much shorter than that of solvation in this solvent ($\langle\tau_{solv}\rangle$ is 26 ps for 1-propanol).[55] However, the lifetime of the ICT state, τ_{ICT}, which represents the lifetime of formation of the TICT state, also shows no correlation with $\langle\tau_{solv}\rangle$ in both kinds of solvents. Hence, it becomes evident that the dynamic Stokes'shift of the maximum of the SE band reveals only the dynamics along the twisting coordinate, not the solvation process. This is also supported by a good correlation between the lifetimes of the LE and ICT states with the viscocity of the solvents.

4.5. Solvent Polarity and Hydrogen-Bonding Effects on the Decay of the S_1 State. It is important to understand the reason for the very strong dependence of the lifetime of the S_1 state of MK in different kinds of solvents (Table 2). Earlier, we reported the lifetime of the S_1 state of MK in two nonpolar solvents, cyclohexane and benzene (6.7 and 25 ps, respectively). In the present work, lifetimes longer than 200 ps have been measured by TCSPC technique. In both aprotc and protic solvents, fluorescence measurements have revealed only single-exponential decay. We observe that in aprotic solvents the lifetime of the S_1 state of MK increases with increase in polarity of the solvent. This can be explained by the fact that, in cyclohexane, the $n\pi^*$ and $\pi\pi^*$ being energetically close to each other, the S_1 state has mixed $\pi\pi^*$ and $n\pi^*$ character, and hence it has a very short lifetime. With increase in polarity of the solvents, the $\pi\pi^*$ state becomes more stabilized compared to the $n\pi^*$ state. In solvents of high polarity, the S_1 state gains pure $\pi\pi^*$ character because the S_1 state is energetically well separated from the higher energy S_2 state with $n\pi^*$ character. Because of the reduction of the $n\pi^*$ character of the S_1 state with increasing polarity, the lifetime increases in more polar solvents. However, the lifetime of the S_1 state increases with decreasing polarity of the alcoholic solvents changing from methanol to octanol. Although Table 2 reveals that τ_{TICT} increases with increasing viscosity of the solvents, no valid explanation can be provided for this kind of dependence. However, τ_{TICT} can be well correlated with the solvent polarity parameter, $E_T(N)$, with reasonable arguments. The decay rates (the inverse of τ_{TICT}) have been plotted as a function of $E_T(N)$ values of the solvents in Figure 13. The $E_T(N)$ values of the solvents, the most popular measure of the electronic solvation, are known to be as much a measure of hydrogen bonding to the solute as a measure of interaction with the solute dipoles.[56−59] In aprotic solvents, the decay rates of the TICT state decrease significantly as the $E_T(N)$ values of the solvents increase. However, in protic solvents, the reverse trend is observed. Increasing the decay rate with increasing $E_T(N)$ values suggests stronger a hydrogen-bonding interaction between the TICT state and the solvent. The stretching frequencies of intermolecular hydrogen bonds act as efficient acceptors of nonradiative energy. This fact possibly explains the weak emissive character of the TICT state of MK in alcohols compared to that in aprotic solvents.

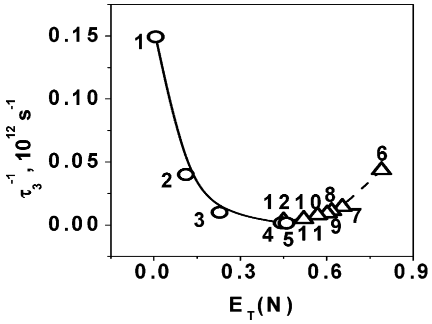

Figure 13. Plot of the decay rates (inverse of τ_3(d), which are given in Table 1) of the TICT kind of the S_1 states of both the conformers as a function of $E_T(N)$ values of the corresponding solvents. The solvents are cyclohexane (1), benzene (2), ethyl acetate (3), acetonitrile (4), DMSO (5), methanol (6), ethanol (7), 1-propanol (8), 1-butanol (8), 1-pentanol (9), 1-octanol (10), and 1-decanol (10). The lifetimes of the S_1 state of MK in cyclohexane (6.7 ps) and benzene (25 ps) are taken from ref 7.

5. Conclusions

Broad and structureless fluorescence spectra of MK in different kinds of solvents have been assigned to the emission from three kinds of states, namely, LE, ICT, and TICT states, and the position of the maximum of the fluorescence band depends on the nature of the solvent, which causes one of the states to be more emissive than the others. Transient absorption measurements in the 470−1000 nm wavelength region with 120-fs time resolution have revealed wavelength-dependent multiexponential and probe-wavelength-dependent relaxation dynamics of the S_1 state of MK in all kinds of solvents because of the overlapping of the ESA and SE spectra of these three kinds of states. Despite this, the kinetic analyses of the temporal profiles recorded at a few selective wavelengths have provided accurate information regarding the lifetimes of these states and revealed the microscopic details of the relaxation dynamics of the S_1 state following photoexcitation of MK. The process of conversion of the LE state to the TICT state has been revealed to be associated with two kinds of twisting motions. Following photoexcitation, the dimethylanilino groups undergo a quick anti-twisting motion about the carbonyl carbon atom to produce a state, called the ICT state, which is actually a resonance-type state with high mesomeric interaction and near-planar geometry. The dimethylamino groups also undergo a twisting motion to about 90° with respect to the plane of the phenyl group to which it is attached. These twisting processes have been found to be the main relaxation processes in the excited state of MK, where solvation seems to play only a minor role. The lifetime of the S_1 state of MK is sensitive to solvent polarity and the hydrogen-bonding abilitiy of the solvents. In nonpolar solvents, the lifetime is too short because of its mixed $n\pi^*$and $\pi\pi^*$ character. Although in polar aprotic solvents the lifetimes are longer because of their pure $\pi\pi^*$ character, in polar protic solvents the lifetimes become shorter in solvents with stronger hydrogen-bonding ability.

Acknowledgment. We are grateful to Professor N. Periasamy of TIFR, Mumbai, for his kind help with the fluorescence lifetime measurements.

Supporting Information Available: Figures showing the temporal evolution of transient absorption following photoexcitation of MK in DMSO, methanol, and ethanol monitored at a few selective wavelengths in sub-100 ps time-domain, following photoexcitation using 400 nm laser pulses of 50 fs duration. Figure showing the temporal profiles of MK in different alcohols recorded up to 450 ps at 490 nm. Figure showing the transient absorption spectra of the TICT state of MK (1) and the anion radicals of MK (2) and DMABP (3) (from ref 51). Table containing the calculated geometrical parameters of the ground state of MK. This material is available free of charge via the Internet at http://pubs.acs.org.

References and Notes

(1) von Veldhoven, E.; Zhang, H.; Rettig, W.; Brown, R. G.; Hepworth, J. D.; Glasbeek, M. *Chem. Phys. Lett*. **2002**, *363*, 189.

(2) Brown, R. G.; Porter, G. *J. Chem. Soc., Faraday Trans*. **1973**, *173*, 1569.

(3) Schuster, D. I.; Goldstein, M. D.; Bane, P. *J. Am. Chem. Soc*. **1977**, *99*, 187.

(4) Liptay, W.; Schumann, H.-J.; Petzke, F. *Chem. Phys. Lett*. **1976**, *39*, 427.

(5) Hoshino, M.; Kogre, M. *J. Phys. Chem*. **1988**, *92*, 417.

(6) Shoute, L. C. T. *Chem. Phys. Lett*. **1992**, *195*, 255.

(7) Singh, A. K.; Palit, D. K.; Mittal, J. P. *Res. Chem. Intermed*. **2001**, *27*, 125.

(8) (a) Groenen, E. J. J.; Koelman, W. N. *J. Chem. Soc., Faraday Trans. 2* **1979**, *75*, 58. (b) Groenen, E. J. J.; Koelman, W. N. *J. Chem. Soc., Faraday Trans. 2* **1979**, *75*, 69.

(9) Klofpper, W. *Chem. Phys. Lett*. **1971**, *11*, 482.

(10) Callis, P. R.; Wilson, R. W. *Chem. Phys. Lett*. **1972**, *13*, 417.

(11) Glasbeek, M.; Zhang, H. *Chem. Rev*. **2004**, *104*, 1929.

(12) Maroncelli, M. *J. Mol. Liq.* **1993**, *57*, 1.

(13) Bhasikuttan, A. C.; Singh, A. K.; Palit, D. K.; Sapre, A. V.; Mittal, J. P. *J. Phys. Chem. A* **1998**, *102*, 3470.

(14) Singh, A. K.; Bhasikuttan, A. C.; Palit, D. K.; Mittal, J. P. *J. Phys. Chem. A* **2000**, *104*, 7002.

(15) Singh, A. K.; Ramakrishna, G.; Ghosh, H. N.; Palit, D. K. *J. Phys. Chem. A* **2004**, *108*, 2583.

(16) Bhasikuttan, A. C.; Palit, D. K. Sapre, A. V.; Mittal, J. P. *J. Phys. Chem. A* **1998**, *102*, 3470.

(17) Singh, A. K.; Palit, D. K.; Mukherjee, T. *J. Phys. Chem. A* **2002**, *106*, 6084.

(18) Grabowski, Z. R.; Rotkiewicz, K.; Rettig, W. *Chem. Rev*. **2003**, *103*, 3899.

(19) Rettig, W.; Maus, M. In *Conformational Analysis of Molecules in Excited States*; Waluk, J., Ed.; Wiley: New York, 2000; p 1.

(20) Rettig, W. *Top. Curr. Chem.* **1994**, *169*, 253.

(21) Palit, D. K.; Singh, A. K.; Bhasikuttan, A. C.; Mittal, J. P. *J. Phys. Chem. A* **2001**, *105*, 6294.

(22) Mokhtari, A.; Fini, L.; Chesnoy, J. *J. Chem. Phys*. **1987**, *87*, 3429.

(23) Nagasawa, Y.; Ando, Y.; Kataoka, D.; Matsuka, H.; Miyasaka, H.; Okada, T. *J. Phys. Chem. A* **2002**, *106*, 2024.

(24) (a) Kovalenko, S. A.; Ernsting, N. P.; Ruthman, J. *Chem. Phys. Lett*. **1996**, *258*, 445. (b) Bingeman, D.; Ernsting, N. P. *J. Chem. Phys*. **1995**, *102*, 2691.

(25) (a) Changenet, P.; Zhang, H.; van der Meer, M. J.; Glasbeek, M.; Plaza, P.; Martin, M. *J. Phys. Chem. A* **1998**, *102*, 6716. (b) Martin, M. M.; Plaza, P.; Meyer, Y.-H.; Badoni, F.; Bourson, J.; Lefevre, J. P.; Valeur, B. *J. Phys. Chem*. **1996**, *102*, 6879. (c) Martin, M. M.; Plaza, P.; Changenet, P.; Meyer, Y.-H. *J. Photochem. Photobiol., A* **1997**, *105*, 197. (d) Martin, M. M.; Plaza, P.; Meyer, Y.-H. *Chem. Phys.* **1995**, *192*, 367. (e) van der Meer, M. J.; Zhang, H.; Glasbeek, M. *J. Chem. Phys.* **2000**, *112*, 2878.

(26) Ramreddy, T.; Sen, S.; Rao, B. J.; Krishnamoorthy, G. *Biochemistry* **2003**, *42*, 12085.

(27) Duxbury, D. F. *Chem. Rev*. **1993**, *93*, 381.

(28) Maruyana, Y.; Ishikawa, M.; Satozano, H. *J. Am. Chem. Soc.* **1996**, *118*, 6257.

(29) Maruyana, Y.; Magniu, O.; Satozano, H.; Ishikawa, M. *J. Phys. Chem. A* **1999**, *103*, 5624.

(30) Sundström, V.; Gilbro, T. *J. Chem. Phys.* **1984**, *81*, 3463.

(31) Korppi-Tommola, J.; Yip, R. W. *Can. J. Chem*. **1981**, *59*, 191.

(32) Luck, H. B.; Mettle, J. L.; Edwards, E. D. *J. Am. Chem. Soc*. **1992**, *114*, 2342.

(33) Foresman, J. B.; Head-Gordon, M.; Pople J. A.; Frisch, M. J. *J. Phys. Chem*. **1992**, *96*, 135.

(34) Schmidt, M. W.; Baldridge, K. K.; Boatz, J. A.; Elbert, S. T.; Gordon, M. S.; Jensen, J. H.; Koseki, S.; Matsunaga, N.; Nguyen, K. A.; Su, S. J.; Windus, T. L.; Dupuis, M.; Montgomery, J. A., Jr. *J. Comput. Chem*. **1993**, *14*, 1347.

(35) Du, M.; Fleming, G. R. *Biophys. Chem*. **1993**, *48*, 101.

(36) (a) Chosrowjan, H.; Mataga, N.; Nakashima, N.; Iamamoto, Y.; Tokunaga, F. *Chem. Phys. Lett*. **1997**, *270*, 267. (b) Changenet, P.; van der Meer, M. J.; Zhang, H.; Hellingwerf. K. J.; Glasbeek, M. *J. Phys. Chem.* **1996**, *100*, 5367.

(37) Sanchez-Galvez, A.; Hunt, P.; Robb, M. A.; Olivucci, Q.; Vreven, T.; Schelgel, H. B. *J. Am. Chem. Soc.* **2000**, *122*, 2911.

(38) Horng, M. L.; Gardecki, J. A.; Papazyan, A.; Maroncelli, M. *J. Phys. Chem.* **1995**, *99*, 2502.

(39) Rettig, W.; Majenz, W. *Chem. Phys. Lett*. **1989**, *154*, 335.

(40) Rettig, W.; Majenz, W.; Lapouyade, R.; Hanke, G. *J. Photochem. Photobiol., A: Chem*. **1992**, *82*, 415.

(41) Sczepan, M.; Rettig, W.; Bicks, Y. L.; Slominski, J. L.; Tolmachev, A. I. *J. Photochem. Photobiol., A: Chem*. **1999**, *124*, 75.

(42) (a) Martin, M. M.; Plaza, P.; Meyer, Y. H. *Chem. Phys.* **1991**, *153*, 297. (b) Martin, M. M.; Plaza, P.; Meyer, Y. H. *J. Phys. Chem.* **1991**, *95*, 9310. (c) Jurczok, M.; Plaza, P.; Chagenet, P.; Meyer, Y. H. *J. Photochem. Photobiol., A: Chem*. **1997**, *105*, 197.

(43) Maus, M.; Rettig, W.; Jonusauskas, G.; Lapouyade, R.; Rulliere, C. *J. Phys. Chem. A* **1998**, *102*, 7393.

(44) Maus, M.; Rettig, W.; Bonafoux, D.; Lapouyade, R. *J. Phys. Chem. A* **1999**, *103*, 3388.

(45) Abraham, E.; Oberle, J.; Jomsauskas, G.; Lapouyade, R.; Rullière, C. *J. Photochem. Photobiol., A: Chem*. **1997**, *105*, 101.

(46) (a) Grabowski, Z. R. In *Supramolecular Photochemistry*; Balzani, V., Ed.; D. Reidel, Publ.: Dordrecht, The Netherlands, 1987; p 319. (b) Dobkowski, J.; Grabowski, Z. R.; Jasny, J.; Zielinski, Z. *Acta Phys. Pol.* **1995**, *A88*, 455.

(47) Rullier, C.; Grabowski, Z. R.; Dobkowski, J. *Chem. Phys. Lett.* **1987**, *137*, 408.

(48) Siemiraczuk, A.; Koput, J.; Pohorille, A. *Z. Naturforsch.* **1982**, *37a*, 598.

(49) Okada, T.; Uesugi, M.; Köhler, G.; Rechthaler, K.; Rotkiewicz, K.; Rettig, W.; Grabner, G. *Chem. Phys.* **1999**, *241*, 327.

(50) Shida, T. *Electronic Absorption Spectra of Radical Ions*; Elsevier: Amsterdam, 1988.

(51) Singh, A. K.; Palit, D. K.; Mukherjee, T. *J. Phys. Chem. A* **2002**, *106*, 6084.

(52) Fleming, G. R. *Chemical Applications of Ultrafast Spectroscopy*; Oxford University Press: New York, 1986; p 186.

(53) Waldeck, W. H. *Chem. Rev.* **1991**, *91*, 415.

(54) Nikowa, L.; Schwarzer, D.; Troe, J.; Schroeder, J. *J. Chem. Phys.* **1992**, *97*, 4827.

(55) Horng, M.; Dahl, K.; Jones, G., II; Maroncelli, M. *Chem. Phys. Lett*. **1999**, *315*, 363.

(56) Marcus, Y. *J. Solution Chem*. **1991**, *20*, 929.

(57) Reichardt, C. *Solvents and Solvent Effects in Organic Chemistry*; VCH Verlagsgesellschaft mbH: FRG, 1990.

(58) Fowler, F. W.; Katritezky, A. R.; Rutherford, R. J. D. *J. Chem. Soc. B* **1971**, *3*, 460.

(59) Reid, P. J.; Alex, S.; Jarzeba, W.; Schlief, R. E.; Johnson, A. E.; Barbara, P. F. *Chem. Phys. Lett*. **1994**, *229*, 93.